Snail: Secure Single Iteration Localization

James Choncholas
Georgia Institute of Technology
Atlanta, USA
jchoncholas3@gatech.edu

Pujith Kachana
Georgia Institute of Technology
Atlanta, USA
pkachana3@gatech.edu

André Mateus
Ericsson Research
Kista, Sweden
andre.mateus@ericsson.com

Gregoire Phillips
Ericsson Research
Sunnyvale, USA
greg.phillips@ericsson.com

Ada Gavrilovska
Georgia Institute of Technology
Atlanta, USA
ada@cc.gatech.edu

ABSTRACT

Localization is a computer vision task by which the position and orientation of a camera is determined from an image and environmental map. We propose a method for performing localization in a privacy preserving manner supporting two scenarios: first, when the image and map are held by a client who wishes to offload localization to untrusted third parties, and second, when the image and map are held separately by untrusting parties. Privacy preserving localization is necessary when the image and map are confidential, and offloading conserves on-device power and frees resources for other tasks. To accomplish this we integrate existing localization methods and secure multi-party computation (MPC), specifically garbled circuits, yielding proof-based security guarantees in contrast to existing obfuscation-based approaches which recent related work has shown vulnerable. We present two approaches to localization, a baseline data-oblivious adaptation of localization suitable for garbled circuits and our novel Single Iteration Localization. Our technique improves overall performance while maintaining confidentiality of the input image, map, and output pose at the expense of increased communication rounds but reduced computation and communication required per round. Single Iteration Localization is over two orders of magnitude faster than a straightforward application of garbled circuits to localization enabling real-world usage in Turbo the Snail, the first robot to offload localization without revealing input images, environmental map, position, or orientation to offload servers.

KEYWORDS

Multi-Party Computation, Localization, Pose Estimation

ACM Reference Format:
James Choncholas, Pujith Kachana, André Mateus, Gregoire Phillips, and Ada Gavrilovska. 2024. **Snail: Secure Single Iteration Localization. In *Proceedings of Proceedings on Privacy Enhancing Technologies.* ACM, New York, NY, USA, 15 pages. https://doi.org/10.56553/popets-2024-0087**

Proceedings on Privacy Enhancing Technologies 2024(3), 446–460

https://doi.org/10.56553/popets-2024-0087

1 INTRODUCTION

Visual localization algorithms allow devices to infer their position in a three-dimensional map from features derived from images. Popular applications include autonomous vehicles, virtual reality, and robotics where a device with a camera is moving through an environment and localizing repeatedly on camera frames to infer its position and orientation over time [1, 15, 36].

Incorporating privacy into visual localization is an active area of research. Consider a lightweight robot equipped with a camera. Privacy preserving localization allows the robot to offload the localization task to more powerful resources without revealing its location, its map, or images taken by its camera. Offloading conserves onboard power and frees resources for other tasks. Privacy is important in this setting because the robot may inadvertently take pictures of sensitive information, or people who do not want their picture taken. Ethical or legal requirements may prevent the images from being shared outside the device domain. Privacy preserving localization also enables settings when the map and camera image are held by different parties, or when both are held by the same party who is trying to prevent data exfiltration by requiring an attacker to compromise multiple systems simultaneously. While technologies have emerged to make privacy preserving localization more efficient, none make formal security statements and many of the claimed security properties have been broken [4, 17, 33, 56].

Previous attempts at secure localization rely on techniques based on obfuscation, like line cloud transformations [56] and adversarial affine subspace embeddings [17]. Such obfuscation-based techniques do not make formal security statements, but they have low overhead and run efficiently. Consequently, these techniques have been shown to be vulnerable to attacks which can recover the input image [10, 47]. Recently, differential privacy has been used to address one such attack however privacy is inversely related to the amount of data processed sequentially [47]. While this is appropriate for some applications, it is not appropriate for repeated invocation, common when localizing on sequential camera frames.

As recent innovation demonstrates, applying privacy-preserving techniques to visual localization that prioritize efficiency over formal security guarantees leaves weaknesses in the protection these techniques afford. At the same time, general purpose secure computation can present performance obstacles with high computation overhead and communication costs. Localization is not well suited to execution under homomorphic encryption due to the algorithm's high multiplicative depth, heavy use of division, and requirement for floating point data representation. Garbled circuits are a better fit for localization, however they are communication intensive. What is needed is a co-design approach that meets privacy expectations with practical efficiency.

In this work, we investigate privacy preserving visual localization using secure multi-party computation (MPC). We first develop a data-oblivious implementation in which we run a standard visual localization algorithm under MPC based on non-linear optimization. This provides the first known implementation of visual localization with formal security guarantees drawn from general purpose secure computation. While secure, this naïve approach has inefficiencies which stem from the iterative nature of localization algorithms. The popular localization approach we consider (minimizing reprojection error via non-linear least squares) is composed of two nested iterative steps which are unfriendly to data-oblivious execution, one being optimization via gradient descent and the other being singular value decomposition (SVD). To address the performance issues these iterative steps present we develop a novel Single Iteration Localization approach, leveraging the fact that localization is typically run repeatedly on sequential camera frames. We modify the outer iterative algorithm, gradient descent, to run each iteration independently in a way which maintains security for a series of localization runs. Then, we address the inner iterative algorithm, the SVD, by finding the optimal number of iterations a priori, which in practice does not depend on secret input data. The resulting *secure, non-linear and iterative localization* – **SNaIL** – runs two orders of magnitude faster than a naïve adaptation of localization to MPC.

In summary, this work makes the following contributions:

- We design a novel Single Iteration Localization (SIL) method for visual localization which increases round complexity in exchange for orders of magnitude runtime improvement and better privacy properties.
- We present a simulation-based definition of security for privacy preserving localization[1].
- We experimentally evaluate SIL against a data-oblivious baseline using two different visual localization algorithms and two different MPC frameworks, EMP [61] and ABY [14].
- We demonstrate real-world practicality with Turbo the Snail, the first robot to offload localization without revealing the view of its camera or its position and orientation in the environment.

2 PRELIMINARIES

This work builds on the goals of previous works seeking to integrate privacy-enhancing features into localization. Our specific focus is the following two privacy goals: 1) preventing image and map reconstruction and 2) maintaining confidentiality of the pose. These two goals represent the most illustrative standards with which to contrast our methods to the existing state-of-the-art [10, 17, 56].

2.1 Secure Computation

Secure computation describes a cryptographic field that seeks to allow multiple parties to compute a function over secret inputs. Secure multiparty computation (MPC) protocols serve a similar purpose as trusted execution environments (TEEs) but do not require hardware support and are not vulnerable to a class of side channel attacks that affect TEEs [28, 29, 59]. When applied in practice, MPC is often collaborative in the sense in that each party has secret inputs to a function, for example a bid in an auction, and the function output, e.g. the winning bid, is learned by all participants. MPC, however, may also be used to offload computation from a weak device to stronger resources such that the weak device with the secret inputs plays a minor role in the protocol.

[1]Source code available at https://github.com/secret-snail/localization-server

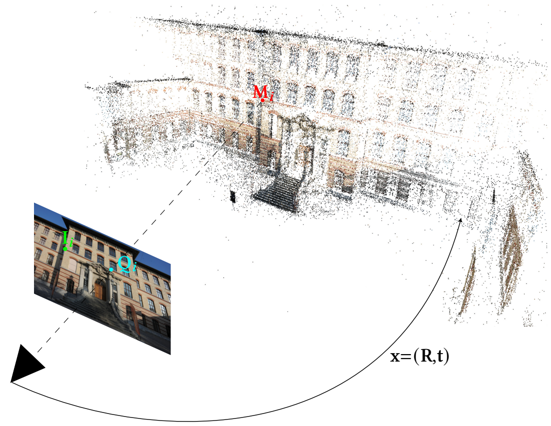

Figure 1: Depiction of the PnP problem. The goal is to find the pose x, which minimizes the error dI = $\|Q_i - I_i\|$ between the image measured points I_i and the map points M_i projected to the image Q_i.

Often MPC protocols are constructed with either Shamir or additive secret sharing protocols [55], else garbled circuit-based protocols [64, 65] briefly introduced next. Secret share-based approaches rely on splitting data into pieces in a way that retains homomorphic properties such that each participant operates on a ciphertext indistinguishable from randomness. Garbled circuit-based approaches instead structure computation as a boolean circuit where each wire value, zero or one, is represented by an encryption key. The circuit is evaluated gate by gate using input wire keys to decrypt output wires which are themselves input keys to the next level of gates. In the two party case, one party plays the role of the generator who creates the garbled circuit and the other party plays the role of the evaluator, decrypting the wires received from the generator. The encryption keys for the first set of wires in the circuit corresponding to plaintext inputs owned by the evaluator are sent using an Oblivious Transfer protocol [49]. This allows the evaluator to learn the appropriate wire label and ensures that generator does not learn which label the evaluator is requesting.

2.2 Visual Localization

Visual localization comprises a series of approaches that infer a device's location from local features extracted from visual data, traditionally derived from a set of 2D or 3D input images depicted in Figure 1. This process commonly employs structure-based approaches, representing scenes through point clouds and feature matching between retrieved 2D images and 3D point clouds. Point clouds, i.e. maps, may be generated using Structure-from-Motion (SfM) [63], constructed simultaneously, or stored from previous mapping of the environment. Such approaches that rely on sharing image features from local 2D images (such as sending them to an external server for analysis) risk leaking private information about the environment to the processing entity, as features are known to be susceptible to image inversion [62]. In practice, several studies demonstrate the recovery of image content from gradient-based feature descriptors, and/or locations, in algorithms such as SIFT [34] and HOG [2], rendering such methods vulnerable to privacy threats when revealed, as one can reasonably reconstruct the image.

Alternatives to such structural approaches exist in the realm of learned localization [33], which replaces part or all of the localization pipeline with machine-learning based optimization. Several emerging families of machine-learning based localization methods demonstrate high degrees of performance comparable or better than image retrieval techniques [16]. However, these learning-based methods currently fail to scale in complexity beyond small and relatively simple scenes [4, 8], and to be as accurate as geometric methods [50]. Furthermore, such methods are comparably vulnerable to image recovery from model features [46].

Classical techniques i.e., non-learning based, to solve the Perspective-n-Point (PnP) problem consist of three main approaches. The first focuses on robust estimation, by removing outliers. A minimal solver is used in conjunction with a RANSAC [20] loop. In the context of camera pose estimation, the minimal number of 2D-3D correspondences required to obtain a solution is three [45]. The second type of approaches solves for the pose using two-steps 1) estimate the 3D points in the camera coordinate system and; 2) solve the 3D-3D pose problem, which has a closed-form solution [58]. An example of this type of approach is presented in [30]. The third type of approach focuses on solving an optimization problem to obtain the pose. Variants of this approach exploit specific problem formulations as in [35], or in specific solvers, such as Levenberg-Marquardt (LM) and Gauss Newton (GN).

In the field of computer vision, the PnP problem [30] consists of estimating the pose (rotation and translation) of a camera with respect to a world coordinate system. The pose is estimated by exploiting a set of 2D feature locations (e.g. points in an image) and their corresponding 3D points (e.g. a 3D map of the environment). If a camera can move freely in 3D space its pose has six degrees of freedom, three rotational and three translational, about the three Cartesian axis. Applications in robotics and AR/VR often use PnP solvers as part of larger processing pipelines including control [9] and mapping [52]. This work focuses only on pose estimation with the PnP problem.

2.3 Privacy-Preserving Localization

Several existing methods implement privacy preserving visual localization and other image query technologies. Speciale et al. [56] introduce a line cloud-based method for localization that relies on transforming 3D point clouds to line clouds to prevent the types of image inversion techniques described in [62]. This work has been extended/adapted to applications in Simultaneous Localization and Mapping (SLAM) [23] and SfM [22] systems. However, the authors note several limitations to the privacy preservation qualities of this method themselves, namely that reconstructing the secret image used as localization input becomes easier with repeated invocation. Chelani et al. [10] further demonstrate additional threats posed by this method that undermine its privacy guarantees in that the secret image can be fully reconstructed in just one invocation. A comparison to this work is shown in Table 1.

Outside of methods directly implementing privacy-preserving localization, other work applies privacy-enhancing technologies to related image query technologies in ways that could be extended to visual localization algorithms. Dusmanu et al. [17] introduce a privacy-preserving method for extracting image features using adversarial affine subspace embeddings. Recently, this approach was shown to be vulnerable to attacks that can recover the input image [47] precluding its use for privacy-preserving localization. The solution proposed to address attacks presented in [47] relies on differential privacy which is not appropriate for the localization setting we consider. Since privacy loss increases with the number of queries, localization on an unchanging sequence of images (like a stationary camera) may quickly exceed a reasonable privacy budget.

Engelsma et al. [18] demonstrate a homomorphically encrypted representation search that could be further adapted to existing visual localization algorithms. This represents a promising frontier, but is currently in the early stages of application and does not scale to such processes in its current form.

The performance envelope of privacy preserving localization proposed in this work is not well suited for time-critical applications like AR/VR, as we later show. There are, however, better suited applications which are less time-sensitive such as Google Visual Positioning System, Facebook Livemaps, and Microsoft Azure Spatial Anchors [24, 40, 41]. These services offer maps supporting localization for thier users. Privacy preserving localization would allow a user to localize an image or video using a mapping service without the user sharing their image or location for privacy reasons, and without the map provider needing to share their map for commercial reasons.

As another example of where privacy is important in localization, consider a delivery robot which must navigate private facilities to deliver packages. The robot is not trusted to learn the full map of these facilities, nor is it allowed to share images it has taken as they may reveal people's faces or confidential information from the facility. Privacy preserving localization keeps images on device and the full map of the facilities off device. The robot may run MPC-based localization with two map servers where one is owned by the robot's manufacturer and the other by the facility who uses their confidential map as input to the protocol. The robot does not learn the full map of the facility, nor do the map servers learn the robot's location or images.

2.4 Homomorphic Encryption and Localization

The localization algorithms considered are particularly challenging to adapt to execution via homomorphic encryption (HE). Most problematic, is that localization is a high depth computation with significant data dependencies between steps. For example, to perform one iteration of Levenberg-Marquardt localization, over 1,000 ciphertext-ciphertext divisions and over 7,000 multiplications are required in a high depth circuit, as we later show in Figure 4. The high degree of dependencies between input data does not suit batching based optimizations for HE schemes popular in BGV, BFV and

	Private Features	Private Map	Private Pose	Round Complexity	Speed
[56]	✗ [10]	✗	✗	1	fastest
[17]	✗ [47]	✗	✗	1	fastest
DO	✓	✓	✓	1	slow
SIL	✓	✓	✓	data dependent	fast

Table 1: Comparison to related privacy preserving localization techniques. DO is our data-oblivious garbled circuits baseline and SIL is our proposed Single Iteration Localization technique.

CKKS where multiple plaintexts are encrypted and operated on together [6, 11, 19]. This, and the large fractional precision required, suggests localization would best suited for a boolean-based FHE scheme. A popular implementation of one such scheme is tfhe-rs which claims to evaluate a boolean gate in 8.5 ms [68]. Given there are 4979 AND and XOR gates per floating point multiplication, for example in EMP-Toolkit's floating point circuits [61], the time required to perform one iteration of Levenberg-Marquardt based localization is estimated to be at least 423 seconds for the multiplications alone. For these reasons, homomorphic encryption is not further considered in favor of an MPC-based approach. While MPC has higher communication complexity than HE, i.e. communication is proportional to the size of the computation vs the size of just the inputs, we later show this cost is practical.

3 SECURITY MODEL

The security guarantees we aim to capture encompass two settings, as previously mentioned. In the first setting, we envision a lightweight client who would like to leverage the resources of two or more capable offload servers. The client has all inputs to the computation, the camera image and 3D map, and does not trust the offload servers with its secret input data. Offloading computation from the client saves power and frees resources for other tasks. In the second setting, the data is instead split between two parties where the input images are known to the client and the map is owned by a third party. The map owner does not want to share the map, but wants to help devices localize using it. For example, a drone using visual localization may be captured thus is not trusted to hold a confidential map, while the map owner should not learn the drone's location or camera images. We consider the semi-honest security model, where participants are not trusted with secrets but are expected to follow the protocol prescribed of them.

While semi-honest security is often considered a stepping stone to more robust security models, even achieving semi-honest security is difficult especially in a performance sensitive setting. The authors of [56] note their line cloud transformations technique is inversely proportional to the amount of data processed in series. It was later discovered that the secret image can be fully reconstructed after just one localization run [10]. This was significant as it showed simply knowledge of which algorithm is used to extract features from the camera's image along with the obfuscated feature coordinates is enough to reasonably recover the image. Due to this, we find it necessary to introduce the more rigorous, simulation-based definition of security for privacy preserving localization. Complexity-based cryptography, or provable security, was first introduced in the context of encryption in 1984 [54]. Schemes considered secure under this definition are sequentially composable: the schemes can be composed without requiring proving that the overall scheme is secure. Given computer vision tasks are often composed e.g. running localization repeatedly on a stream of camera frames or in combination with random sample consensus algorithms, we choose this framework in which to define security for privacy preserving localization.

In MPC, security against semi-honest adversaries is formulated as a game referred to as the real-ideal paradigm. Informally, there is an attacker who runs a protocol and remembers all the messages they receive and send. If another algorithm called a simulator can generate a convincing set of messages that resembles what a real attacker would see during protocol execution without actually running the protocol, the scheme is considered secure. Next we define this game more formally in the context of localization using notation and format from Lindell [32, Chapter-6, Section-4.2]. The inputs to localization, namely the set of features taken from an image and from a map, as well as the output pose are considered secret, though the secret map features may be owned by the device or another party. This definition considers a streaming model where multiple poses are computed from a set of images and maps. We note that localization algorithms are deterministic (nonrandomized) by nature which allows for a slightly simpler definition of security as the output can always be computed from inputs alone and thus parties in the protocol may be simulated individually.

- Let $l(\mathbf{I}, \mathbf{M}, x)$ be a probabilistic deterministic polynomial-time localization algorithm which takes as input a set of $\mathbf{I} = \{\mathbf{i}_0, \ldots, \mathbf{i}_{i-1}\}$ image feature locations, a set $\mathbf{M} = \{\mathbf{m}_0, \ldots, \mathbf{m}_{i-1}\}$ map feature locations, and initial pose estimate $\mathbf{x}$. l returns a refined pose, $\mathbf{x}_{\text{refined}}$.
- Let $L(\mathbf{F})$ compute l on every member of a set of j image features, map features, and initial pose estimates $\mathbf{F} = \{\{\mathbf{I}, \mathbf{M}, \mathbf{x}\}_0, \ldots, \{\mathbf{I}, \mathbf{M}, \mathbf{x}\}_{j-1}\}$.
- Let π be an n-party protocol which computes L. The view of the k-th party during an execution of π is $\text{view}_k^{\pi}(\mathbf{F}) = (w, r^k; m_0^k, \ldots, m_h^k)$ where w is the party's input, r^k is the k-th party's randomness, and m_n^k represents the n-th message that it received. The output of π to party k is output_k and is implicitly part of the party's view because π is deterministic.

Protocol π securely computes L in the presence of static, semi-honest adversaries if there exists probabilistic polynomial-time algorithms $S_0, \ldots, S_{n-1}$ such that

$$\{S_k(1^\kappa, w_k, \text{output}_k)\}_{\mathbf{F},\kappa} \stackrel{c}{\equiv} \{\text{view}_k^{\pi}(\mathbf{F})\}_{\mathbf{F},\kappa} \tag{1}$$

where, the symbol $\stackrel{c}{\equiv}$ refers to computational indistinguishability with security parameter κ. Given the two views, the probability they can be distinguished by a non-uniform polynomial-time algorithm is negligible, i.e. $O(\frac{1}{2^\kappa})$.

This definition has some differences compared to a straight forward application of simulation-based definition of security from generic MPC. First, this definition considers a "streaming" model where multiple poses are computed from a set of images and maps

F. The streaming model captures temporal dimension where localization is executed multiple times sequentially. This is a common real-world setting for localization where a device is continuously localizing on a stream of images from a camera, as in robotics, AR/VR, etc. Directly applying the standard definition of security to localization would require each localization execution to be simulated independently. The streaming model however supports more efficient protocols, as we later show with our Single Iteration Localization approach, because localization executions do not need to be independent. From a security perspective, it is sufficient that a sequence of localization executions do not leak any information about their inputs, but simulating each independently is unnecessary.

This definition gives insight into where previous privacy preserving localization attempts have failed. Line cloud transformations of Speciale et. al. cannot be simulated; the lines contained within the view are not known to the simulator and thus the difference between the real and simulated views can be easily distinguished, as practically proven by Chelani et. al. [10, 56]. Granted, line clouds were only meant to prevent image reconstruction and do not attempt to hide map feature locations **M** or the output pose **x** (see Table 1). However, just considering input feature locations, an adaptation of the above definition to remove the map **M** and output pose **x** still suggests line cloud transformations are not secure. Furthermore, line cloud transformations do not consider the streaming model; authors note their technique is inversely proportional to the amount of data processed in series. A concrete definition of security is needed to capture repeated invocation via a streaming model to avoid this leakage.

4 OVERVIEW OF PRIVACY PRESERVING LOCALIZATION

Our primary contribution is a practical method and implementation of privacy preserving localization $L(\mathbf{F})$ on a set of image and map features **F** meeting the security definition in §3. This requires overcoming two types of challenge, the first being practical challenges stemming from the large size and depth of the computation required. Secondly, is addressing the iterative nature of localization, for which we introduce Single Iteration Localization. But first, we introduce localization as a functionality.

Algorithm 1 Pose Estimation

Inputs: Image feature locations **I**,
Map feature locations **M**,
Initial pose estimate **x**.
Output: Pose $\mathbf{x}_{\text{refined}} = l(\mathbf{I}, \mathbf{M}, \mathbf{x})$.

This work considers privacy preserving localization in two contexts. The first is a client-server setting where a lightweight client wishes to offload localization to more capable servers, e.g. when the client is a mobile device with limited power or computational resources. In this setting, the client encrypts its input image and map features and sends them to the offload servers. The offload servers compute on the ciphertext and each returns a ciphertext representing the result back to the client. The client can then construct the plaintext resultant pose including position and orientation $x = l(\mathbf{I}, \mathbf{M})$. Both input features and output pose are considered confidential in contrast to related approaches in which only the input features are secret [56]. The offload servers are expected to be within different administrative domains, for example two providers offering private localization as a service. The details of how data is sent to and retrieved from offload servers depends on the underlying MPC protocol, covered later, however at a high level, protocols based on secret shares split input data into additive pieces while garbled circuit protocols send inputs encoded as circuit wire labels.

The second setting considered is where a client holds the features extracted from their image **I**, but the 3D map **M** is held by a third party. The client and third party interact to compute the pose. The client should not learn anything about the map other than what can be inferred from the pose, and the third party should learn (informally) nothing. In the real world, the full map $\mathbf{M}_{\text{full}}$ likely contains more features than the client's image **I**. In order to keep $\mathbf{M}_{\text{full}}$ confidential, we assume the existence of an alignment functionality to match the client's features in **I** to the subset of features shared by the map $\mathbf{M}_{full}$, specifically, $\mathbf{M} = align(\mathbf{I}, \mathbf{M}_{full})$. We believe the alignment functionality is a reasonably straightforward application of private information retrieval [12] and leave concrete instantiation to future work. When alignment is composed with localization, i.e. $x = l(\mathbf{I}, \text{align}(\mathbf{I}, \mathbf{M}_{\text{full}}))$, the client learns neither the exact map features **M**, nor map features which did not have a corresponding image feature, i.e. $\{x : x \in \mathbf{M}_{\text{full}} \text{ and } x \notin \mathbf{M}\}$.

In both settings considered, the core challenge to instantiating l in a privacy preserving way is in addressing the iterative nature of localization. Iterative algorithms like localization are not friendly to running under MPC because they are not data-oblivious, meaning control flow depends on secret data i.e. the convergence criteria. To run an iterative algorithm under MPC, an upper bound of iterations must be specified a priori, regardless of convergence at runtime, to ensure the rate of convergence is not leaked. If the rate of convergence were leaked, it reveals sensitive information allowing the devices position to be inferred, especially when localization is run repeatedly like on sequential camera frames (as is common in robotics, AR/VR, and autonomous vehicles). The iteration leakage problem has been studied previously in the context of privacy preserving SAT solvers [37, 57] and there is no direct solution; an upper bound of iterations must be executed to hide the real number of iterations required for convergence. Localization is particularly problematic as it contains an outer gradient descent iterative algorithm, each iteration of which computes the singular value decomposition (SVD) to (pseudo) invert a matrix which is itself an iterative algorithm. Our Single Iteration Localization approach addresses this, instantiated using an appropriate localization algorithm and MPC protocol given the context.

We have identified two key observations to address the wasted work required by the iterative localization algorithm considered. The first key is when computing the SVD: our analysis shows the number of iterations required does not in fact depend on the input data in the case of the considered localization algorithm. As such, the optimal number of SVD iterations can be fixed a priori, which turns out to be data-independent and wastes no work. The second key is to execute each iteration of the outer gradient decent algorithm independently. Doing so is secure under the assumption that a certain number of localization executions will be run in series, as we later show more formally. This turns out to be quite amenable to how localization is run in practice. In the context of autonomous vehicles, robotics, AR/VR, etc. localization is invoked repeatedly on sequential camera frames. Thus, with these observations and algorithm-cryptography co-design, we then demonstrate practicality of our approach with Turbo the Snail, a proof of concept robot which securely offloads localization to navigate its environment.

5 DESIGN

The design of a privacy preserving localization method for MPC concerns four critical choices: selecting an appropriate localization algorithm, an MPC protocol and implementation, a data representation, and addressing issues with data-obliviousness given the iterative nature of optimization-based localization. The design is presented in this order as each choice is dependent on the previous. Design choices are justified them in terms of their wall clock runtime and security implications, where applicable.

5.1 Localization Algorithm

The vast number of localization algorithms is at odds with the significant engineering effort required to build them in privacy preserving frameworks. This process is time-consuming as algorithms must be re-written from scratch to use privacy preserving data types, be made data-oblivious, and correctly stage data in and out of the privacy preserving framework. Thus, this work considers only the most popular approach to localization consisting of solving a non-linear least-squares problem which minimizes the reprojection error [26]. Specifically, find the pose $\mathbf{x}$ (position and orientation) which minimizes the error $\mathbf{dI}$ between the set of projected image points $\mathbf{Q} = \text{proj}(\mathbf{x}, \mathbf{M})$, and the corresponding measured image points $\mathbf{I}$. $\mathbf{M} = [\mathbf{x}^M, \mathbf{y}^M, \mathbf{z}^M]^\top$ is the set of 3D map points. Notice the one-to-one correspondence between each point in $\mathbf{M}$ and $\mathbf{I}$, i.e., for each 3D point in the map, we can observe it in the image, a measured 2D point. Formally, the problem is defined as

$$\arg\min_{\mathbf{x}} \sum_{i=1}^{n} \mathbf{dI}^2, \text{ with } \mathbf{dI} = \|\mathbf{Q}_i - \mathbf{I}_i\|, \tag{2}$$

where n is the number of 2D and 3D points. Subscript i denotes the ith point $\mathbf{Q}_i = [x_i^Q, y_i^Q]$ projected into the image plane from 3D point $\mathbf{M}_i = [x_i^M, y_i^M, z_i^M]^\top$ and similarly for the i'th measured image point $\mathbf{I}_i = [x_i^I, y_i^I]$.

Point projection is computed with intrinsic camera parameters (focal length $\mathbf{f} = [f_x, f_y]$ and image center $\mathbf{c} = [c_x, c_y]$), pose $\mathbf{x}$ (represented as Euler finite rotation matrix $\mathbf{R}$, and translation $\mathbf{t} = [t_x, t_y, t_z]^\top$), and 3D world point $\mathbf{M}_i$ as

$$proj(\mathbf{x}, \mathbf{M}_i) = \begin{bmatrix} f_x & 0 & c_x \\ 0 & f_y & c_y \\ 0 & 0 & 1 \end{bmatrix} \begin{bmatrix} r_{1,1} & r_{1,2} & r_{1,3} & t_x \\ r_{1,1} & r_{2,2} & r_{2,3} & t_y \\ r_{3,1} & r_{3,2} & r_{3,3} & t_z \end{bmatrix} \begin{bmatrix} x_i^M \\ y_i^M \\ z_i^M \\ 1 \end{bmatrix}, \tag{3}$$

where r_{ij} represent the entries of $\mathbf{R}$ at row i and column j. A depiction of the PnP problem in presented in Fig. 1. For a detailed explanation of 3D point projection refer to [38, Section 3.3].

To solve the non-linear least-squares problem, we consider two optimization algorithms: Gauss-Newton (GN) and Levenberg- Marquardt (LM) with Fletcher's improvement [21]. The pose update $\mathbf{dx}$ for each is defined as

$$\begin{aligned} &\text{GN: } \mathbf{dx} = (\mathbf{J}^\top \mathbf{J})^{-1} \mathbf{J}^\top \mathbf{dI} \\ &\text{LM: } \mathbf{dx} = \left(\mathbf{J}^\top \mathbf{J} + \lambda \text{ diag}(\mathbf{J}^\top \mathbf{J})\right)^{-1} \mathbf{J}^\top \mathbf{dI}, \end{aligned} \tag{4}$$

where the Jacobian matrix $\mathbf{J}$ is computed numerically from the right-hand side of Equation (3) by perturbing each element of the pose by epsilon using a one hot encoded vector and projecting the points using the perturbed pose. The reprojection error $\mathbf{dI}$ is computed as the difference between the projected image points $\mathbf{Q}$ and the measured points $\mathbf{I}$. LM is presented at a high level in Algorithm 2 with a more detailed description in reference [42]. Note Algorithm 2 computes the pose for a single image and map $l(\mathbf{I}, \mathbf{M})$, while this work is concerned with pose estimation for a sequence of images and maps $L(\mathbf{F})$ as described by the security model in §3.

Algorithm 2 Levenberg-Marquardt Pose Estimation

Inputs: Image features $\mathbf{I}$, Map features $\mathbf{M}$,
Initial pose estimate $\mathbf{x}$.
Public Parameters: Intrinsic camera parameters $\mathbf{f}$ and $\mathbf{c}$.
Convergence criteria c, Fletcher's λ.
Output: Refined pose $\mathbf{x}_{\text{refined}} = l(\mathbf{I}, \mathbf{M}, \mathbf{x})$.

```
while not converged do
    Q ← proj(x, M)                                  ▷ Point projection
    for each degree of freedom d ← 1, 6 do          ▷ Jacobian
        J[:][d] ← ∂/∂x_d proj(x + (one_hot_d ∗ ε), M),
    end for
    dI ← Q_i − I_i                                  ▷ Reprojection error
    dx ← (JᵀJ + λ diag(JᵀJ))^(−1) JᵀdI
    x ← x + dx                                      ▷ Pose update
    if Σ_{i=1}^{n} ||dI||² ≤ c then                 ▷ Convergence criteria
        Converged. Output x.
    end if
end while
```

LM is selected for its wide popularity, real-world usage, and generality as it is the default PnP algorithm in OpenCV [5] and accepts any number of input point correspondences making it useful in combination with other localization related tasks like RANSAC [20]. GN is considered as it requires the same set of linear algebra operations as LM, thus is easy to implement, and also requires fewer matrix multiplications at the cost of inverting a larger matrix. While there are many more algorithms, LM and GN are the most popular and require a narrow variety of operations, i.e., matrix arithmetic (2), point projection (3), Euler finite rotation transformation (3), and a matrix (pseudo) inverse via SVD (4). Furthermore, these algorithms can be directly applied, or easily adjusted, to other computer vision problems like relative pose estimation [3], homography & image alignment [26], and Structure-from-Motion (SfM) [52].

5.2 MPC Library

This work compares localization algorithms implemented using two MPC libraries secure in the semi-honest setting, ABY and EMP. ABY is a flexible MPC library which performs secure computation using arithmetic, boolean, and Yao's garbled circuits [14]. ABY is flexible in that it supports switching between protocols to allow the

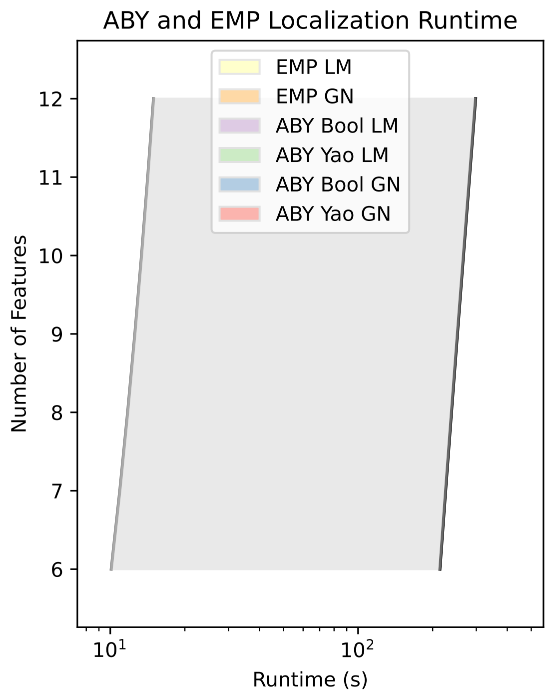

Figure 2: Time to localize using ABY and EMP secure computation frameworks on feature data from ETH3D [53]. Each measurement is an average of three trials using randomly selected points. The same random sequence of points are used across measurements. Note the log scale of the x-axis. The highlighted area is the difference between the slowest EMP configuration and the fastest of ABY.

most efficient protocol to be used for differnt parts of a computation. EMP, on the other hand, is a framework with many protocols, one of which is a highly efficient garbled circuits implementation of the semi-honestly secure half-gates protocol and optimizations [27, 67]. One major difference between these implementations that is not immediately clear is ABY pre-generates circuits before executing them while EMP generates and executes garbled circuits on the fly. Circuit pre-generation has the disadvantage in that large circuits require large amounts of memory. Running our data-oblivious LM-based localization with 6 input correspondences and default security parameter results in out of memory errors consuming over 100 GB of RAM (including swap) in ABY. EMP on the other hand completes using less than 1 GB of RAM.

While ABY and EMP's garbled circuits have similar theoretical performance, in practice the lightweight nature of EMP gives it a significant advantage for this application, as shown in Figure 2. ABY's circuit pre-generation means that circuit structure can be re-used after being built in contrast with EMP's on-the-fly style execution. This is an artifact of the MPC framework and not the underlying protocols. However, only considering the online time of ABY and ignoring all setup costs like base oblivious transfer and circuit generation, ABY is still two orders magnitude slower than the total runtime of EMP due to the impact of the library's heavy utilization of the memory allocator.

This finding is surprising because in theory the two frameworks rely on similar garbled circuits protocols yet runtime varies widely. Simply measuring the number of gates in a localization circuit and multiplying by the time it takes to evaluate a single logic gate is not an accurate way to estimate the runtime of frameworks which pre-generate circuits. The impact of ABY's memory allocations reduces the performance of the framework regardless of protocol, be it boolean or Yao. Note ABY's arithmetic protocol is not of interest in this context because localization requires operating on floating point data types, as later discussed. We suspect there are optimizations we could make to our ABY implementation like aggregating operations across multiple integers to amortize certain cryptographic overheads and switching between Arithmetic, Boolean, and Yao protocols dynamically, however, this optimization process is even more time-consuming than the initial implementation within the privacy preserving framework and it is unlikely to make up the orders of magnitude difference to EMP. As such, further analysis only considers EMP.

5.3 Data Representation

Given promising results from using alternative ways to represent data in the field of machine learning, we consider various representations in privacy preserving localization [25, 31]. Plaintext arithmetic operations on floating point data are accelerated on modern hardware making localization on floating point data fast (around 10 ms for 10k operations) and thus other representations like fixed point are not usually considered. In contrast, when performing floating point operations under the MPC frameworks considered, there are no floating point functional units. Garbled circuit logic gates are evaluated in the same manner no matter how data is represented. For this reason we consider both fixed and floating point data types of various width for privacy preserving localization.

Pose estimation is typically computed with double precision floating point therefore the first question is whether localization is possible using single precision floats and fixed point. The second question is then of performance. For measurement purposes we use the ETH3D dataset [53], a 3D map and series of images taken from known locations commonly used to measure accuracy and performance of PnP solvers. Due to integer over/underflow, localization with 32-bit fixed point precision is not possible. On the other hand, 64-bit fixed point localization does converge but only when the SVD, a sub-step in both GN and LM, is computed with floating point. While even larger width fixed point representations may allow the SVD to converge successfully, performance measurements suggest even 64-bit fixed point is not useful.

Even though fixed point arithmetic is simpler than floating, comparing 64-bit fixed point (the smallest width fixed point representation for which localization converges) to 32-bit floating is not a clear performance win due to the increase in data width. In Figure 3 we see 64-bit fixed point addition is faster than 32-bit floating point but multiplication is slower. This is expected as addition has linear complexity in the number of bits while multiplication has quadratic. Thus, determining which offers better performance for localization requires knowledge of how many of each operation are performed.

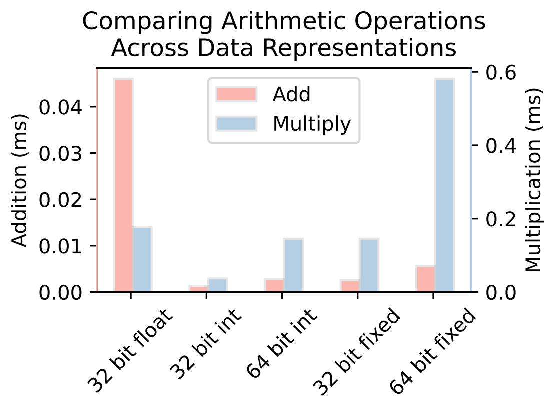

Figure 3: Time to perform addition and multiplication using floating point and fixed point data representation of various width with EMP's semi-honestly secure half-gates protocol.

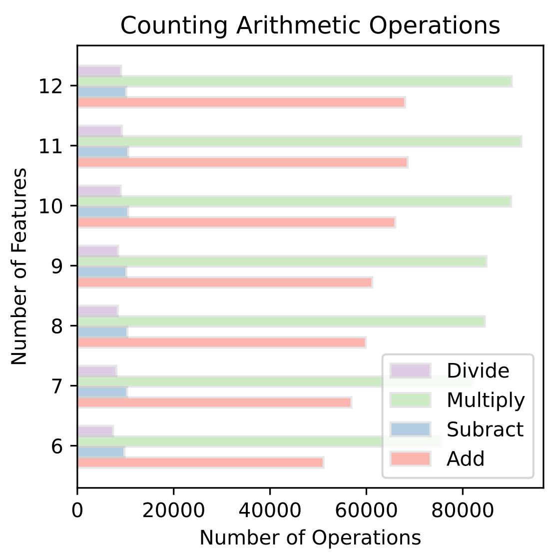

Figure 4: Arithmetic operations performed during LM localization using Single Iteration Localization. GN exhibits similar behavior.

Figure 4 shows multiplication is the dominant operation in both LM and GN localization, thus it is fastest to compute with floating point representation. From these results, we project operations using 64-bit fixed point to be over three times slower than 32-bit floating. We also notice 64-bit fixed point converges 90% less frequently than 32-bit floating point on the ETH3D dataset, suggesting even wider data types may be necessary to achieve similar convergence properties to 32-bit floating point. Due to this performance degradation, we do not further analyze the impact of fixed point on localization accuracy or the rate of convergence. We leave the exploration of alternative floating point representations to future work e.g. half precision or bfloat16 [60], as they have more general implications to plaintext localization.

5.4 Garbled Circuits for Computation Offload

Garbled circuit protocols are often considered to run between two parties, each of which has secret inputs to the function being computed. In the offload setting we consider, instead the offload servers have no inputs to the function and are not allowed to learn the output. Achieving this requires some minor logistical modifications to the garbled circuits protocol setup.

Recall two party garbled circuit protocols have two roles, a generator and an evaluator. The generator creates garbled circuit, which in practice mostly consists of repeatedly evaluating the AES blockcipher. The garbled circuit, i.e. a set of ciphertexts, is then sent to the evaluator who decrypts parts of the received ciphertext, a process that again mostly consists of evaluating AES. The evaluator learns a subset of the ciphertext representing inputs called input wire labels via a primitive named oblivious transfer. The evaluator then uses the input wire labels to decrypt the garbled circuit.

In the setting where all plaintext inputs and outputs are owned by the client, for whom we additionally want to minimize computation and network usage, the simplest way to get the correct input wire labels from generator to evaluator is to have the generator send all labels to the client, who then forwards the appropriate label per wire onwards to the evaluator. We make a slight optimization from the above approach to reduce the bandwidth requirements of the client. The client chooses a random seed and sends it to the generator who uses a pseudorandom function and the seed to create the wire labels for the garbled circuit. Note that the EMP toolkit framework already uses a seeded PRF to generate the garbled circuit for performance reasons (/dev/random is slow); we have instead allowed the client to choose this seed which is not an issue since the client is the only party who supplies the secret input. After, the generator creates the garbled circuit, they send it to the evaluator excluding the input wire labels. The client, knowing the circuit seed, can generate the input wire labels without interaction and send them to the evaluator. The circuit is evaluated as usual and the output labels are sent back to the client who can decode their plaintext meaning. This saves the client from needing to receive all wire labels from the generator. Instead, the client may generate them directly and send to the evaluator. Since the same seed is used to generate input wire labels and the rest of the garbled circuit, correctness holds. Note in the case of EMP and the half-gates protocol, the client must also know the global circuit delta [27] as part of the generation process. Intuitively, it is okay for the client to learn the seed and delta as the client is the only party who supplies secret inputs and is allowed to learn the output. While this is appropriate for the offload setting, in the setting where the input image and map are known to different parties, this optimization is not appropriate.

6 SINGLE ITERATION LOCALIZATION

The localization algorithms considered (i.e. Algorithm 2) are iterative by nature; they run a sequence of gradient descent steps until convergence is reached. Furthermore, each iteration requires computing the (pseudo) inverse of a matrix which is itself an iterative

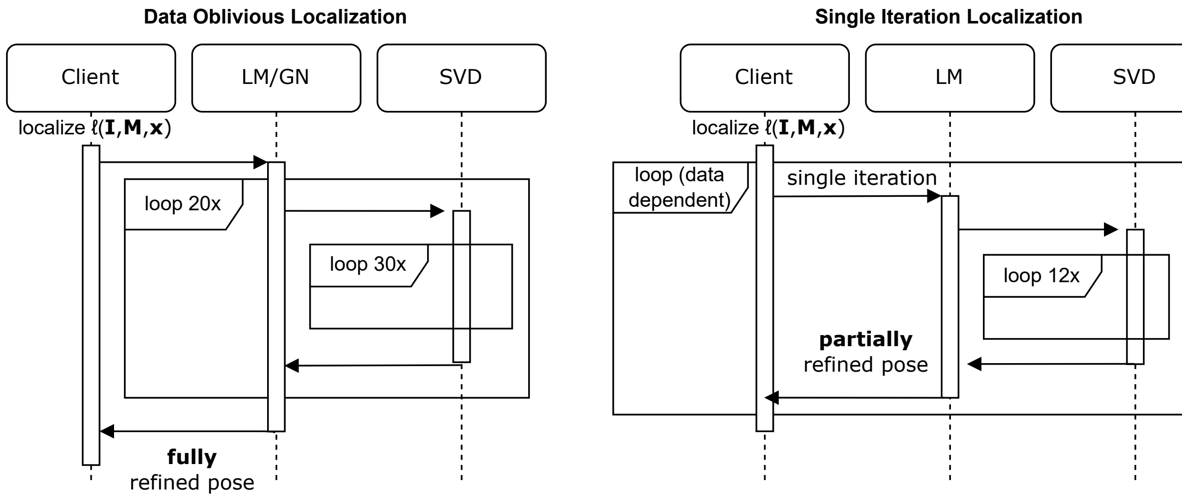

Figure 5: UML diagrams of a naïve data-oblivious adaptation of PnP localization via gradient descent and Single Iteration Localization. On the left, a constant upper bound of optimization iterations (default of 20 LM iterations in OpenCV) are required. On the right, the number of optimization iterations is data-dependent which in practice is much fewer than 20 but comes at the cost of additional round complexity. Regarding the inner SVD algorithm, the number of iterations can be reduced from a constant upper bound on the left (default of 30 in Eigen/LAPACK) to the optimal number (12) on the right using public knowledge about the input distribution, namely two QR sweeps per singular value and one singular value for each physical degree of freedom (2*6).

process when using the popular algorithm from Demmel and Kahan [13], used in the Eigen and LAPACK libraries to reduce the bidiagonal form to singular values. Executing such iterative algorithms in a data-oblivious setting (like under MPC) have a critical drawback: a fixed number of iterations must be executed regardless of the rate of convergence. Either work is wasted by running more than necessary iterations, or completeness of the solution is degraded by running too few.

Our approach maintains the invariant that control flow does not depend on secret data but avoids wasting work by running on multiple inputs. The outer iterative algorithm, LM optimization via gradient decent, is broken apart such that each step runs independently. Then, stringing the steps from multiple localizations together hides the convergence rate of each individual localization. The inner algorithm, the SVD, is addressed through finding that in practice there is a constant and optimal of number of iterations which does not depend on secret data. We call the combination of the two techniques Single Iteration Localization.

Concerning the outer gradient decent algorithm, instead of running the entire decent under MPC, we run each optimization step individually, hence the name Single Iteration Localization. Specifically, instead of running LM optimization until the pose meets the convergence criteria, SIL takes a single gradient descent step towards the optimal pose and returns the intermediate result, as shown in Figure 5. The client can then decide after each step if convergence has been met and can refine the pose by running SIL with the same image and map. When convergence has been met, they may provide a new image and map and start to localize with the new inputs. The MPC parties cannot tell whether the client is refining the pose from the previous step or if they are computing the first step for a new image, because of the security guarantees of the MPC protocol. This approach requires that there is a stream of images to localize on. If the client were to only localize a single image, the offload servers would learn how many iterations it takes to compute the pose which is a security issue as previously discussed. Since localization is often evaluated repetitively on a sequence of camera frames, repeated evaluation is desirable in practice. Later in §7 we better quantify how many images constitutes a stream and the security properties.

There is still one remaining problem in SIL as described. A single gradient descent step requires inverting a matrix which is itself an iterative algorithm whose convergence is data-dependent. Just as before, this suggests an upper bound of iterations is required however the previous solution to reduce the number of iterations does not work as this problem is nested within the previous. It turns out there is an optimal number of iterations which is constant and known beforehand, and thus is easy to encode in the garbled circuit. To see why, we describe more about how the SVD of a matrix is computed, the underlying operation in matrix inversion. To compute the SVD of a matrix it is first reduced to an upper bidiagonal form using Householder transformations. Then, the SVD is computed from the bidiagonal matrix using QR factorization, eliminating the upper diagonal entries as it sweeps across the diagonal in an iterative fashion. The number of iterations taken to reduce the bidiagonal form to singular values depends on the values of the matrix being decomposed. A general rule of thumb is two QR sweeps per singular value [44, p. 165,] but a bidiagonal matrix whose diagonal entries are equal to the superdiagonal takes fewer QR factorization iterations [13, Table 2.] The key insight we rely on is that the number of singular values of the matrix is always six as each corresponds to a physical degree of freedom. The question is then if localization algorithms require inverting a matrix which, after householder transformations (the first step in computing the SVD), result in diagonal entries equal to the superdiagonal. The geometric implication of this phenomenon with respect to localization is not immediately clear, however, for every experiment performed including real world images and those from the ETH3D dataset, there are no cases where a single diagonal entry is within $\pm 10^{-5}$ of the superdiagonal, much less all diagonal entries. If there is a case where more QR sweeps are required, the accuracy of the localization may be affected, however, this suggests the number of iterations required to compute the SVD is a constant known ahead of time. Namely, twelve QR sweeps are required for convergence, two for each singular value, and there are six singular values each corresponding to a physical degree of freedom. The takeaway is that the *fixed upper bound* of iterations required to compute the SVD can be set as the optimal number of iterations which in practice does not depend on the secret inputs.

As we later quantify, Single Iteration Localization is faster than executing one large garbled circuit for each localization run when considering a stream of images, however it comes at the cost of additional round complexity. Instead of participants interacting once per image to share a garbled circuit, they must instead do so for every intermediate gradient decent step. In practice round complexity is not an issue as connectivity is already assumed. Furthermore, the network RTT time is much faster than the time to run one iteration, so the effect of the additional rounds is minimal.

6.1 Implementation

As a baseline, we have implemented a data-oblivious adaptation of the localization algorithms described in §5.1. The baseline maintains the invariant that control flow does not depend on secret data, thus an upper bound of iterations is encoded for each of the iterative routines, namely gradient descent and SVD. The upper bounds are taken from the plaintext algorithms, e.g. the plaintext LM algorithm from OpenCV runs at most 20 iterations, and the plaintext LAPACK SVD algorithm runs at most 30 iterations. The baseline is visualized in Figure 5 and has been implemented for GN and LM localization, in both the EMP and ABY frameworks.

We compare the baseline against Single Iteration Localization, also implemented for GN and LM in both ABY and EMP in C++, all of which are available under the MIT license[2]. The ABY implementation is 3,887 lines of code, EMP is 1,924 lines, and reference plaintext implementation used for automated testing is 848 lines. Each implementation is an independent library that includes all necessary linear algebra operations depending only on the respective MPC library, including MPC-based adaptations of the SVD algorithm from Demmel and Kahan [13].

7 EVALUATION

Our evaluation is focused on both security and performance. Because this work leverages existing localization algorithms, we do not discuss plaintext-related metrics like localization accuracy, ability to converge, or sensitivity to noise as the privacy preserving implementations share these properties with plaintext algorithms which have been studied extensively [7].

7.1 Security Analysis of Single Iteration Localization

This security analysis considers an MPC-hybrid model meaning we assume the underlying garbled circuit protocol is secure and prove security of Single Iteration Localization according to the definition in §3. This implies the input feature locations, map, and pose remain confidential over a single iteration, as it is simply an invocation of garbled circuits which we assume is secure. It may seem like assuming the MPC protocol is secure leaves nothing left to prove, however, this is not the case. Simply running each iteration of gradient decent under MPC independently to localize *one* image is not secure as the number of invocations is leaked. The important question is regarding security in the streaming setting, i.e. over multiple invocations of localization.

As an example, suppose a client has one image which requires 8 localization iterations to converge. The MPC participants learn how many times they were called and in turn have learned something about the quality of the initial pose estimate. In general, more iterations are required if the initial pose estimate is far away from the true pose; fewer are required if the initial pose estimate is nearby. Convergence speed also depends on tunable algorithm parameters and the presence of degenerate solutions in the path of gradient descent. It is unclear if such information could be used to directly reconstruct the input image similar to attacks on line cloud obfuscation in previous work [10, 56]. What is clear, however, is this leakage has a negative impact on a higher level notion of privacy over time. For example, a camera moving through an area which is easier to localize compared to the rest of its environment requires fewer iterations in one specific area. The MPC participants learn when the client is in the easily-localized area and when it is not. This leakage is captured by the definition in Equation (1), namely, the view of participants does not contain j which is the size of $\mathbf{F}$ (the number of images and maps). This leakage is critical to address and is primary focus of our security analysis.

Recall the key insight of Single Iteration Localization is to break each iteration of gradient descent apart. To estimate the pose of a single image, SIL must be invoked repeatedly, until the pose converges. If computing the pose of one image, this would still reveal the number of invocations to the MPC participants, which is a security problem as previously discussed. But if computing the pose on a stream of images, the MPC participants cannot tell which pose refinement iterations belong to which images. This hides how many iterations were required to converge for each image. If the MPC participants also do not know how many images were used as input, they cannot infer the number of iterations per image, which addresses the leakage. Decoupling the number of iterations from the higher level localization executions is the key to security.

There is one issue with the security argument as described. We have not quantified how many images count as a "stream" or more specifically, how many times SIL must be invoked to hide the association of gradient decent steps to input images. For example, a stream containing one single image which requires three gradient

[2] https://github.com/secret-snail/localization-server

decent iterations to compute the pose doesn't offer very good security properties because the MPC participants can see only three iterations were performed and so the initial pose estimate must have been very close to the true pose. It turns out, it depends on a public parameter of the LM and GN localization algorithms, namely the upper bound on the number of gradient decent steps. OpenCV's implementation of LM localization defines a maximum number of iterations of 20 meaning if the pose hasn't converged after 20 iterations, localization will halt. It follows that if at least 20 iterations are performed, the probability of an adversary outputting the correct number of iterations per image is no better than guessing.

More generally, if SIL is invoked o times and the publicly known upper bound of iterations is c, the number of images which could have been used as input is between $\frac{o}{c}$ and o (where $o > c$). Thus, the probability of an adversarial offload server A correctly outputting the number of input images i from the number of iterations it ran, o, is given by:

$$\Pr[\mathrm{A(o) = i}] < \frac{1}{o - \frac{o}{c}} + \frac{1}{p(\kappa)} \qquad (5)$$

where $p(\kappa)$ is a polynomial in security parameter κ, an artifact which appears due to the negligible advantage an attacker has when distinguishing garbled circuit wire labels. Thus, we conclude that Single Iteration Localization is secure when invoked a minimum of c times. In practice, the default maximum from OpenCV is $c = 20$ and since localization is often called repeatedly (more than 20 times) on camera frames, this is not a difficult requirement to meet.

Next, we prove security of Single Iteration Localization in the simulation-based definition from Equation (1) using the notation from §3. The proof follows trivially from the previous discussion.

LEMMA 7.1. *SIL securely implements localization* $\mathbf{L}$ *over a set of image and map feature sets* $\mathbf{F}$ *in the presence of static semi-honest adversaries in the MPC-hybrid model when invoked more than* c *times.*

PROOF. Simulator S constructs a view for the offload server by running one iteration of localization l on randomly chosen inputs $\mathbf{I}$, and $\mathbf{M}$, appending messages of the party's respective role to the view. The messages for each iteration of l may be simulated given we consider the MPC-hybrid model. The simulator does this a random number times which is at least c. The sets of messages corresponding each iteration are indistinguishable from one another and from those in the real protocol, thus the two ensembles are indistinguishable. □

There are two important takeaways. First, the more often the client calls the localization function, the stronger the privacy up to a maximum of c iterations which may be fully simulated. This is the opposite of prior work where privacy guarantees weaken with subsequent invocations. Second, the security guarantees of SIL are in fact stronger than a naïve data-oblivious adaptation. The latter reveals exactly how many input images were used for localization. SIL reveals only a probability distribution of how many input images were used as input $[o, \frac{o}{c}]$.

In summary, Single Iteration Localization does not reveal any information about the input features (both image and map), or the pose when run more than c times in series which in practice is 20. This is true for any input including the case when the same input image and map is repeating (corresponding to a stationary camera) or for inputs that change over time (a moving camera). Previous attacks on privacy preserving localization rely on exploiting knowledge of the feature locations to reconstruct the input image. Such attacks are not possible on Single Iteration Localization as the image features, map features, and all other partial information remains confidential.

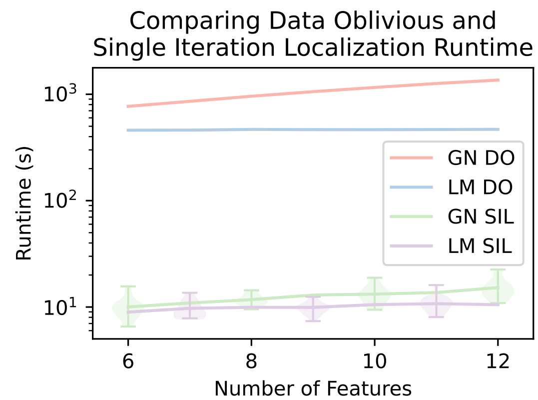

Figure 6: Time to compute localization using data oblivious and Single Iteration Localization with EMP. Data oblivious uses a fixed upper-bound of 20 optimization iterations (the default number of LM iterations in OpenCV) and 30 SVD iterations (the default in LAPACK) where as Single Iteration Localization is data dependent.

7.2 Performance Evaluation

Server side performance is evaluated using a desktop with an 11th generation Intel® core-series CPU. Each MPC participant is a process on the test machine communicating over localhost where bandwidth is limited to 2.5 Gbps and latency is introduced artificially where noted using traffic control. The rationale for 2.5 Gbps being it is the maximum theoretical bandwidth of WiFi 6E, the latest standard at the time of writing. Localization is performed on features from the ETH3D dataset [53] where each measurement is an average of randomly selected points where the same random sequence is used across measurements. Measurements for which convergence was not achieved are not included in the results (in these cases the plaintext implementation also did not converge). Reported times are wall clock and implementations are not multithreaded due to their high bandwidth requirements as later shown.

The performance advantage of Single Iteration Localization over the data oblivious baseline are between two and three orders of magnitude as shown in Figure 6. It is natural to see why running fewer iterative steps under MPC reduces runtime, but the magnitude of this difference has implications for the future of applying general purpose secure computation to localization. Localization with six points takes 11 seconds to compute rising modestly with small increases in input size. While 11 seconds is not within a practical envelope for low latency localization applications like AR, it is practical for certain robotics applications, as we later demonstrate.

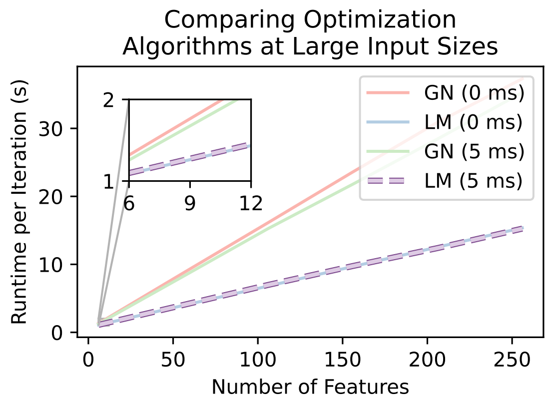

(a) Wall clock runtime of Single Iteration Localization on large input size with 0 ms and 5 ms of latency introduced between offload servers.

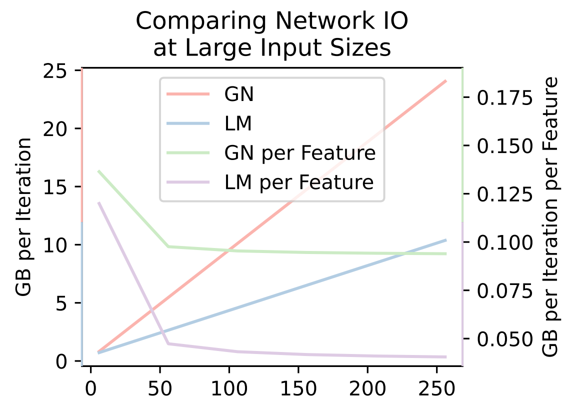

(b) Average number of bytes transmitted between offload servers (from garbled circuit generator to evaluator) when computing Single Iteration Localization. Bytes from evaluator to generator are negligible.

Figure 7: Comparison on large input size of Levenberg-Marquardt (LM) and Gauss Newton (GN) localization with EMP using Single Iteration Localization. The heavy cost of large input sizes highlights the importance of input preprocessing to reduce the number of input point correspondences. Inset axis show such small input sizes between 6 and 12 point correspondences. Values are normalized with respect to number of iterations to remove dependence on input data and algorithm tunable parameters.

Next, we consider network communication between *client* and offload servers for the client-server computation offload setting. EMP, being based on the half-gates garbled circuits protocol [67], shares secret inputs via a correlated oblivious transfer protocol. Localization is a unique case where neither generator nor evaluator (the two roles in the protocol the offload servers play) have the secret input data as they are computing on behalf of a client. The natural approach to garbled circuits is the generator sends all wire label pairs to the client, who then forwards the appropriate label from the pair, based on their secret bits, to the evaluator. This requires the client receive 2κ bits per input bit and send κ bits per input bit where κ is a security parameter, the size of the wire labels (128 bits by default in EMP's semi-honest protocol). In the case of six input point correspondences and EMP's default security parameters, this amounts to the client sending 123 Kb and receiving 246 Kb. We improve upon this by noticing if the client knows the global circuit delta (a part of the free XOR optimization [27]), and circuit seed, they may generate labels for the evaluator themselves. From a security perspective this is not an issue, as the client is considered a trusted third party and is allowed to learn all inputs and outputs of the computation in the offload setting we consider. The seed based approach reduces data the client receives to a constant 2κ bits (circuit delta and seed) while data sent remains κ bits per input bit (wire labels). In the case of six input point correspondences this amounts to 123 Kb of total communication instead of 369 Kb (123 + 246) via the natural approach.

7.3 Limitations

Thus far, performance has been evaluated on small input sizes, between six and twelve input point correspondences. While this range is representative of small input sizes for the localization methods considered and is used by other work [51], the quality of localization can increase with larger input sizes notably when input data is noisy. Feature detection algorithms like SIFT [34] typically extract many more features, around 1000 points per image, but the number which can be matched to 3D map features is typically lower. Thus, we consider the performance of input sizes up to 256 points which is reasonable for popular feature detection algorithms. Prior localization work considers between 100 and 300 points [48]. Figure 7a focuses on the interaction between the two offload servers, namely how latency affects runtime and the relationship between input size and network communication.

Localization even on small input sizes takes around 10 seconds to compute, which likely precludes time-sensitive applications like AR/VR because the displacement distance, or error accumulated in the pose as estimated by less accurate means, grows beyond what is acceptable before the more accurate pose may be computed. This makes Single Iteration Localization better suited for less time sensitive applications like robotics or offline processing, for example those described in §2.3.

Comparing the scalability of GN to LM, both algorithms invert a matrix on every optimization iteration; the key difference is the size of the matrix each inverts. GN computes the pseudo-inverse of a $2n \times 6$ Jacobian matrix $\mathbf{J}$ where n is the number of input point correspondences and each row represents the partial derivative with respect to one degree of freedom in the pose. LM instead inverts a 6×6 matrix ($\mathbf{J}^\top \mathbf{J}$ plus an offset along the diagonal from [21]). Because of the performance impact of inverting large matrices, LM is expected to perform better than GN on large inputs. This behavior is not explicitly clear for small numbers of points shown in Figure 6, but becomes important as the input size scales as shown in Figure 7a. Because LM also outperforms GN on small input sizes, LM is in general the better approach. We see each LM iteration of SIL takes roughly 20 seconds to compute on 256 input points in Figure 7a. Assuming 8 iterations to converge (a realistic value observed in the ETH3D dataset), localization completes in 160 seconds.

Given MPC protocols are communication-intensive by nature, we measure the bytes sent between the two MPC participants in Figure 7b. Localization using 256 points using GN sends almost 200 GB while LM sends 64 GB, again assuming 8 iterations required for convergence. In the client-server offload setting, this communication is between the two offload servers and does not involve the device, however, in the multi-party setting where input data is distributed between the parties, this high communication cost is a limiting factor precluding large input sizes.

In Single Iteration Localization, we propose executing each iteration of the outer gradient descent algorithm independently. We argue this approach is secure if invoked a minimum number of times, a number which depends on a public parameter of the plaintext algorithm, as discussed in §7.1. This is amenable to repeated invocation however it could be seen as a limitation of in the case where a single or few input images must be localized using a large stream size. In this case, however, SIL is no slower than the naïve data-oblivious adaptation and still benefits from running fewer SVD iterations driven by the analysis in §6.

The performance envelope and high network requirements of the proposed methods are such that localization is best performed using a small number of high quality feature correspondences. As such, applying these methods likely requires input pre-processing to eliminate outlier or even unnecessary inlier point correspondences.

Before continuing, we briefly mention performance related to trusted execution environments (TEEs) like Intel® SGX. Memory requirements to perform localization on the number of points considered is small enough to fit into secure enclaves, thus we expect performance in TEEs to be near native (plaintext) speed, making Single Iteration Localization orders of magnitude slower than the 10s of milliseconds required to compute in the clear. The "sluggish" performance of MPC compared to TEE reflects the cost of eliminating side channels, reducing requirements for specialized hardware, and eliminating trust required of hardware vendors.

7.4 Proof of Concept: Turbo the Snail

To demonstrate the feasibility of privacy preserving localization, we built a Raspberry Pi-based robot acting as a lightweight client which offloads localization. The robot is equipped with one RGB camera and uses its onboard WiFi module to communicate with the offload servers, a maximum bandwidth of 100 Mbps. The robot is programmed to move to a target location defined within its environment, leveraging the AprilTag library [43] to detect marker images printed on paper in its environment. The marker corners are detected in the camera image and then matched to a ground truth 3D map of the marker's position, yielding the 2D and 3D features used in localization. Once the pose is known, the robot moves to a predefined target position using position-based visual servoing [9] via the ViSP library [39].

In this configuration, the servers learn neither the input feature locations (2D nor 3D), nor the resultant pose. By using few high quality input point correspondences, the number of features is kept low. The use of specific markers or patterns is commonly used in visual servoing [9]. Since privacy preserving localization takes roughly ten seconds to complete on eight input points as seen in Figure 6, we allow the robot to move 0.1 meters before relocalizing and thus, moves at a rate of 0.01 m/s, hence its form – a snail. We find in practice the snail moves more quickly because the pose estimate from one localization is used as the initial estimate for the next, reducing the number of optimization iterations required. After the initial pose is solved, convergence is frequently achieved in only one call to SIL.

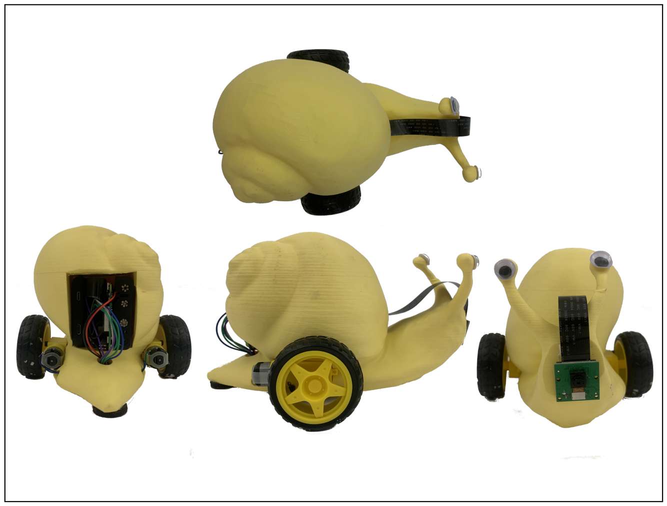

Figure 8: Robotic snail proof of concept. Model adapted from [66].

In the context of localization, power consumption is an important metric as devices are often mobile and battery powered. To quantify this, the servo motors of the robot are disabled and pose estimation is performed every 20ms. In the case of Single Iteration Localization, the offload servers return dummy data such that the rate of localization may be compared to that of plaintext. Energy consumed by the Raspberry Pi model 3B+ is measured with a TP-Link K115 energy monitor. Offloading localization reduces power consumption from 3.7 Watts to 2.8 Watts (24%) with idle power being 1.7 Watts. We attribute the increase between idle and SIL mostly to polling the socket while waiting for data to be received from the offload servers, presenting an opportunity for future optimization.

8 CONCLUSION

In this work we introduce a simulation-based definition of security for privacy preserving localization, and Single Iteration Localization (SIL) a secure approach to visual localization. While SIL requires additional rounds of communication, it reduces the computation and communication required per round by running each localization iteration independently. We then demonstrate the practicality of SIL with Turbo, the privacy preserving snail.

ACKNOWLEDGMENTS

Thank you anonymous shepherd and reviewers. This work has been supported by NSF awards CCF-2217070 and CNS-1909769.

REFERENCES

[1] Fernando A Auat Cheein, Natalia Lopez, Carlos M Soria, Fernando A di Sciascio, Fernando Lobo Pereira, and Ricardo Carelli. 2010. SLAM algorithm applied to robotics assistance for navigation in unknown environments. *Journal of Neuroengineering and Rehabilitation (JNER)* 7, 1 (2010), 1–16.

[2] Vassileios Balntas, Karel Lenc, Andrea Vedaldi, and Krystian Mikolajczyk. 2017. HPatches: A benchmark and evaluation of handcrafted and learned local descriptors. In *IEEE Conf. Computer Vision and Pattern Recognition (CVPR)*. 5173–5182.

[3] Adrien Bartoli and Peter Sturm. 2004. Nonlinear estimation of the fundamental matrix with minimal parameters. *IEEE Trans. Pattern Analysis and Machine Intelligence (T-PAMI)* 26, 3 (2004), 426–432.

[4] Eric Brachmann and Carsten Rother. 2021. Visual camera re-localization from RGB and RGB-D images using DSAC. *IEEE Trans. Pattern Analysis and Machine Intelligence (T-PAMI)* (2021).

[5] G. Bradski. 2000. The OpenCV Library. *Dr. Dobb's Journal of Software Tools* (2000).

[6] Zvika Brakerski, Craig Gentry, and Vinod Vaikuntanathan. 2012. (Leveled) Fully Homomorphic Encryption Without Bootstrapping. In *Innovations in Theoretical Computer Science Conference (ITCS)*. 309–325.

[7] Joao Campos, Joao R Cardoso, and Pedro Miraldo. 2019. POSEAMM: A unified framework for solving pose problems using an alternating minimization method. In *IEEE Int'l Conf. Robotics and Automation (ICRA)*. 3493–3499.

[8] Tommaso Cavallari, Luca Bertinetto, Jishnu Mukhoti, Philip Torr, and Stuart Golodetz. 2019. Let's take this online: Adapting scene coordinate regression network predictions for online RGB-D camera relocalisation. In *Int'l Conf. 3D Vision (3DV)*. 564–573.

[9] François Chaumette and Seth Hutchinson. 2006. Visual servo control. I. Basic approaches. *IEEE Robotics & Automation Magazine (RA-M)* 13, 4 (2006), 82–90.

[10] Kunal Chelani, Fredrik Kahl, and Torsten Sattler. 2021. How Privacy-Preserving are Line Clouds? Recovering Scene Details from 3D Lines. In *IEEE Conf. Computer Vision and Pattern Recognition (CVPR)*. 15668–15678.

[11] Jung Hee Cheon, Andrey Kim, Miran Kim, and Yongsoo Song. 2017. Homomorphic Encryption for Arithmetic of Approximate Numbers. In *Int'l Conference on the Theory and Applications of Cryptographic Techniques (Asiacrypt)*.

[12] Benny Chor, Eyal Kushilevitz, Oded Goldreich, and Madhu Sudan. 1998. Private Information Retrieval. *Journal of the ACM (JACM)* (1998).

[13] James Demmel and William Kahan. 1990. Accurate singular values of bidiagonal matrices. *SIAM Journal on Scientific Computing (SISC)* 11, 5 (1990), 873–912.

[14] Daniel Demmler, Thomas Schneider, and Michael Zohner. 2015. ABY-A framework for efficient mixed-protocol secure two-party computation. In *Network and Distributed System Security Symposium (NDSS)*.

[15] Kaichang Di, Qiang Zhao, Wenhui Wan, Yexin Wang, and Yunjun Gao. 2016. RGB-D SLAM based on extended bundle adjustment with 2D and 3D information. *Sensors* 16, 8 (2016), 1285.

[16] Mihai Dusmanu, Ignacio Rocco, Tomas Pajdla, Marc Pollefeys, Josef Sivic, Akihiko Torii, and Torsten Sattler. 2019. D2-net: A trainable cnn for joint description and detection of local features. In *IEEE Conf. Computer Vision and Pattern Recognition (CVPR)*. 8092–8101.

[17] Mihai Dusmanu, Johannes L Schonberger, Sudipta N Sinha, and Marc Pollefeys. 2021. Privacy-preserving image features via adversarial affine subspace embeddings. In *IEEE Conf. Computer Vision and Pattern Recognition (CVPR)*. 14267–14277.

[18] Joshua J Engelsma, Anil K Jain, and Vishnu Naresh Boddeti. 2022. Hers: Homomorphically encrypted representation search. *IEEE Transactions on Biometrics, Behavior, and Identity Science (T-BIOM)* (2022).

[19] Junfeng Fan and Frederik Vercauteren. 2012. Somewhat Practical Fully Homomorphic Encryption. Cryptology ePrint Archive, Paper 2012/144. https://eprint.iacr.org/2012/144.

[20] Martin A Fischler and Robert C Bolles. 1981. Random sample consensus: a paradigm for model fitting with applications to image analysis and automated cartography. *Commun. ACM* 24, 6 (1981), 381–395.

[21] Roger Fletcher. 1971. A modified Marquardt subroutine for non-linear least squares. (1971).

[22] Marcel Geppert, Viktor Larsson, Pablo Speciale, Johannes L Schönberger, and Marc Pollefeys. 2020. Privacy preserving structure-from-motion. In *European Conf. Computer Vision (ECCV)*. 333–350.

[23] Marcel Geppert, Viktor Larsson, Pablo Speciale, Johannes L Schonberger, and Marc Pollefeys. 2021. Privacy Preserving Localization and Mapping from Uncalibrated Cameras. In *IEEE Conf. Computer Vision and Pattern Recognition (CVPR)*. 1809–1819.

[24] Google. 2019. Google Visual Positioning Service. https://blog.research.google/2019/02/using-global-localization-to-improve.html?m=1.

[25] Suyog Gupta, Ankur Agrawal, Kailash Gopalakrishnan, and Pritish Narayanan. 2015. Deep learning with limited numerical precision. In *Int'l Conf. Machine learning (ICML)*. PMLR, 1737–1746.

[26] R. I. Hartley and A. Zisserman. 2004. *Multiple View Geometry in Computer Vision* (second ed.). Cambridge University Press.

[27] Vladimir Kolesnikov and Thomas Schneider. 2008. Improved garbled circuit: Free XOR gates and applications. In *Int'l Colloquium on Automata, Languages and Programming (ICALP)*. Springer, 486–498.

[28] Jaehyuk Lee, Jinsoo Jang, Yeongjin Jang, Nohyun Kwak, Yeseul Choi, Changho Choi, Taesoo Kim, Marcus Peinado, and Brent ByungHoon Kang. 2017. Hacking in darkness: Return-oriented programming against secure enclaves. In *USENIX Security Symposium*. 523–539.

[29] Sangho Lee, Ming-Wei Shih, Prasun Gera, Taesoo Kim, Hyesoon Kim, and Marcus Peinado. 2017. Inferring fine-grained control flow inside {SGX} enclaves with branch shadowing. In *USENIX Security Symposium*. 557–574.

[30] Vincent Lepetit, Francesc Moreno-Noguer, and Pascal Fua. 2009. Epnp: An accurate O(n) solution to the pnp problem. *Int'l J. Computer Vision (IJCV)* 81, 2 (2009), 155–166.

[31] Bernd Lesser, Manfred Mücke, and Wilfried N Gansterer. 2011. Effects of reduced precision on floating-point SVM classification accuracy. *Procedia Computer Science* 4 (2011), 508–517.

[32] Yehuda Lindell. 2017. *Tutorials on the Foundations of Cryptography: Dedicated to Oded Goldreich*. 277–346 pages.

[33] Xingcheng Liu, Shaohua Su, Feng Han, Yitong Liu, and Zhihong Pan. 2018. A range-based secure localization algorithm for wireless sensor networks. *IEEE Sensors Journal* 19, 2 (2018), 785–796.

[34] David G Lowe. 2004. Distinctive image features from scale-invariant keypoints. *Int'l J. Computer Vision (IJCV)* 60 (2004), 91–110.

[35] C-P Lu, Gregory D Hager, and Eric Mjolsness. 2000. Fast and globally convergent pose estimation from video images. *IEEE Trans. Pattern Analysis and Machine Intelligence (T-PAMI)* 22, 6 (2000), 610–622.

[36] Weixin Lu, Yao Zhou, Guowei Wan, Shenhua Hou, and Shiyu Song. 2019. L3-net: Towards learning based lidar localization for autonomous driving. In *IEEE Conf. Computer Vision and Pattern Recognition (CVPR)*. 6389–6398.

[37] Ning Luo, Samuel Judson, Timos Antonopoulos, Ruzica Piskac, and Xiao Wang. 2022. {ppSAT}: Towards {Two-Party} Private {SAT} Solving. In *USENIX Security Symposium*. 2983–3000.

[38] Yi Ma, Stefano Soatto, Jana Košecká, and Shankar Sastry. 2004. *An invitation to 3-d vision: from images to geometric models*. Vol. 26.

[39] E. Marchand, F. Spindler, and F. Chaumette. 2005. ViSP for visual servoing: a generic software platform with a wide class of robot control skills. *IEEE Robotics & Automation Magazine (RA-M)* 12, 4 (2005), 40–52.

[40] Meta. 2019. Facebook Live Maps. https://tech.facebook.com/reality-labs/2019/9/inside-facebook-reality-labs-research-updates-and-the-future-of-social-connection/.

[41] Microsoft. 2020. Microsoft Azure Spatial Anchors. https://azure.microsoft.com/en-us/products/spatial-anchors.

[42] Jorge Nocedal and Stephen J Wright. 1999. *Numerical optimization*. Springer.

[43] Edwin Olson. 2011. AprilTag: A robust and flexible visual fiducial system. In *IEEE Int'l Conf. Robotics and Automation (ICRA)*. 3400–3407.

[44] Beresford N Parlett. 1998. *The symmetric eigenvalue problem*. SIAM.

[45] Mikael Persson and Klas Nordberg. 2018. Lambda twist: An accurate fast robust perspective three point (P3P) solver. In *European Conf. Computer Vision (ECCV)*. 318–332.

[46] Francesco Pittaluga, Sanjeev J Koppal, Sing Bing Kang, and Sudipta N Sinha. 2019. Revealing scenes by inverting structure from motion reconstructions. In *IEEE Conf. Computer Vision and Pattern Recognition (CVPR)*. 145–154.

[47] Francesco Pittaluga and Bingbing Zhuang. 2023. LDP-Feat: Image Features with Local Differential Privacy. arXiv:2308.11223

[48] Tong Qin, Peiliang Li, and Shaojie Shen. 2018. Vins-mono: A robust and versatile monocular visual-inertial state estimator. *IEEE Trans. Robotics (T-RO)* 34, 4 (2018), 1004–1020.

[49] Michael O Rabin. 1981. How to Exchange Secrets with Oblivious Transfer. *Technical Report TR-81, Aiken Computation Laboratory, Harvard University* (1981).

[50] Torsten Sattler, Qunjie Zhou, Marc Pollefeys, and Laura Leal-Taixe. 2019. Understanding the limitations of cnn-based absolute camera pose regression. In *IEEE Conf. Computer Vision and Pattern Recognition (CVPR)*. 3302–3312.

[51] Thomas Schneider, Marcin Dymczyk, Marius Fehr, Kevin Egger, Simon Lynen, Igor Gilitschenski, and Roland Siegwart. 2018. maplab: An open framework for research in visual-inertial mapping and localization. *IEEE Robotis and Automation Letters (RA-L)* 3, 3 (2018), 1418–1425.

[52] Johannes L Schonberger and Jan-Michael Frahm. 2016. Structure-from-motion revisited. In *IEEE Conf. Computer Vision and Pattern Recognition (CVPR)*. 4104–4113.

[53] Thomas Schops, Johannes L Schonberger, Silvano Galliani, Torsten Sattler, Konrad Schindler, Marc Pollefeys, and Andreas Geiger. 2017. A multi-view stereo benchmark with high-resolution images and multi-camera videos. In *IEEE Conf. Computer Vision and Pattern Recognition (CVPR)*. 3260–3269.

[54] Goldwasser Shafi and Micali Silvio. 1984. Probabilistic encryption. *J. Comput. System Sci.* 28, 2 (1984), 270–299.

[55] Adi Shamir. 1979. How to share a secret. *Commun. ACM* 22, 11 (1979), 612–613.

[56] Pablo Speciale, Johannes L Schonberger, Sudipta N Sinha, and Marc Pollefeys. 2019. Privacy preserving image queries for camera localization. In *IEEE Int'l Conf.*

Computer Vision (ICCV). 1486–1496.
[57] Tomas Toft. 2009. Solving linear programs using multiparty computation. In *Int'l Conference on Financial Cryptography and Data Security*. 90–107.
[58] Shinji Umeyama. 1991. Least-squares estimation of transformation parameters between two point patterns. *IEEE Trans. Pattern Analysis and Machine Intelligence (T-PAMI)* 13, 04 (1991), 376–380.
[59] Jo Van Bulck, Nico Weichbrodt, Rüdiger Kapitza, Frank Piessens, and Raoul Strackx. 2017. Telling Your Secrets without Page Faults: Stealthy Page {Table-Based} Attacks on Enclaved Execution. In *USENIX Security Symposium*. 1041–1056.
[60] Shibo Wang and Pankaj Kanwar. 2019. BFloat16: The secret to high performance on Cloud TPUs. https://cloud.google.com/blog/products/ai-machine-learning/bfloat16-the-secret-to-high-performance-on-cloud-tpus. Accessed: 2022-04-01.
[61] Xiao Wang, Alex J. Malozemoff, and Jonathan Katz. 2016. EMP-toolkit: Efficient MultiParty computation toolkit. https://github.com/emp-toolkit.
[62] Philippe Weinzaepfel, Hervé Jégou, and Patrick Pérez. 2011. Reconstructing an image from its local descriptors. In *IEEE Conf. Computer Vision and Pattern Recognition (CVPR)*. 337–344.
[63] Yang Yang, Yixu Song, Fangwen Zhai, Zhaozhou Fan, Yue Meng, and Jiaxin Wang. 2009. A high-precision localization algorithm by improved SIFT key-points. In *Int'l Congress on Image and Signal Processing (CISP)*. 1–6.
[64] Andrew C Yao. 1982. Protocols for secure computations. In *Foundations of Computer Science*. 160–164.
[65] Andrew Chi-Chih Yao. 1986. How to generate and exchange secrets. In *Foundations of Computer Science*. 162–167.
[66] zacleung. 2017. Snail model. https://www.thingiverse.com/thing:2202789/files. Accessed: 2022-03-23.
[67] Samee Zahur, Mike Rosulek, and David Evans. 2015. Two halves make a whole. In *Int'l Conference on the Theory and Applications of Cryptographic Techniques (Eurocrypt)*. 220–250.
[68] Zama. 2022. TFHE-rs: A Pure Rust Implementation of the TFHE Scheme for Boolean and Integer Arithmetics Over Encrypted Data. https://github.com/zama-ai/tfhe-rs.